ADF 951 257

(2)

AD-A206 328

TECHNICAL REPORT RD-RE-88-5

THE CURRENT TECHNOLOGICAL STATUS OF SPATIAL LIGHT MODULATORS

Tracy D. Hudson
Research, Development, and Engineering Center
Redstone Arsenal, AL 35898-5248

AUGUST 1988

U.S. ARMY MISSILE COMMAND
Redstone Arsenal, Alabama 35898-5000

SMI FORM 1021, 1 AUG 85 PREVIOUS EDITION IS OBSOLETE

DISPOSITION INSTRUCTIONS

DESTROY THIS REPORT WHEN IT IS NO LONGER NEEDED. DO NOT RETURN IT TO THE ORIGINATOR.

DISCLAIMER

THE FINDINGS IN THIS REPORT ARE NOT TO BE CONSTRUED AS AN OFFICIAL DEPARTMENT OF THE ARMY POSITION UNLESS SO DESIGNATED BY OTHER AUTHORIZED DOCUMENTS.

TRADE NAMES

USE OF TRADE NAMES OR MANUFACTURERS IN THIS REPORT DOES NOT CONSTITUTE AN OFFICIAL INDORSEMENT OR APPROVAL OF THE USE OF SUCH COMMERCIAL HARDWARE OR SOFTWARE.

UNCLASSIFIED
SECURITY CLASSIFICATION OF THIS PAGE

REPORT DOCUMENTATION PAGE

Form Approved
OMB No 0704-0188
Exp Date Jun 30, 1986

1a REPORT SECURITY CLASSIFICATION: UNCLASSIFIED		1b RESTRICTIVE MARKINGS		
2a SECURITY CLASSIFICATION AUTHORITY		3 DISTRIBUTION/AVAILABILITY OF REPORT: Approved for public release; distribution is unlimited.		
2b DECLASSIFICATION/DOWNGRADING SCHEDULE				
4 PERFORMING ORGANIZATION REPORT NUMBER(S): TR-RD-RE-88-5		5 MONITORING ORGANIZATION REPORT NUMBER(S)		
6a NAME OF PERFORMING ORGANIZATION: Research Directorate Res, Dev, & Eng Center	6b OFFICE SYMBOL (If applicable): AMSMI-RD-RE	7a NAME OF MONITORING ORGANIZATION		
6c ADDRESS (City, State, and ZIP Code): Commander U.S. Army Missile Command ATTN: AMSMI-RD-RE Redstone Arsenal, AL 35898-5248		7b ADDRESS (City, State, and ZIP Code)		
8a NAME OF FUNDING/SPONSORING ORGANIZATION	8b OFFICE SYMBOL (If applicable)	9 PROCUREMENT INSTRUMENT IDENTIFICATION NUMBER		
8c ADDRESS (City, State, and ZIP Code)		10 SOURCE OF FUNDING NUMBERS: PROGRAM ELEMENT NO.	PROJECT NO	TASK NO / WORK UNIT ACCESSION NO

11 TITLE (Include Security Classification)
THE CURRENT TECHNOLOGICAL STATUS OF SPATIAL LIGHT MODULATORS

12 PERSONAL AUTHOR(S)
Tracy D. Hudson

13a TYPE OF REPORT	13b TIME COVERED	14 DATE OF REPORT (Year, Month, Day)	15 PAGE COUNT
Final	FROM OCT 87 TO APR 88	August 1988	34

16 SUPPLEMENTARY NOTATION

17 COSATI CODES			18 SUBJECT TERMS (Continue on reverse if necessary and identify by block number)
FIELD	GROUP	SUB-GROUP	Spatial Light Modulators; Matched Filtering; Optical Computing; Pattern Recognition

19 ABSTRACT (Continue on reverse if necessary and identify by block number)

The major technological obstacle to optical computing and optical pattern recognition is the performance of spatial light modulators. This report is an attempt to present a realistic outlook for the future of optical computing by briefly presenting the basics of promising modulators with regard to their response times, resolution, and cost.

20 DISTRIBUTION/AVAILABILITY OF ABSTRACT: ☐ UNCLASSIFIED/UNLIMITED ☒ SAME AS RPT ☐ DTIC USERS	21 ABSTRACT SECURITY CLASSIFICATION: UNCLASSIFIED
22a NAME OF RESPONSIBLE INDIVIDUAL: Tracy D. Hudson	22b TELEPHONE (Include Area Code): (205) 876-7687 / 22c OFFICE SYMBOL: AMSMI-RD-RE

DD FORM 1473, 84 MAR — 83 APR edition may be used until exhausted. All other editions are obsolete

SECURITY CLASSIFICATION OF THIS PAGE
UNCLASSIFIED

ACKNOWLEDGMENTS

The author would like to express his greatest appreciation to Dr. Don A. Gregory and Mr. David J. Lanteigne, both of the Research Directorate, for their knowledge, support, and encouragement during this investigation.

TABLE OF CONTENTS

LIST OF FIGURES

I. INTRODUCTION

A major technological hurdle for optical computing and optical pattern recognition is the current state of performance of Spatial Light Modulators (SLMs). A SLM is a device that yields an image in coherent light from either an incoherent light or electrical signal input. The slow response, low resolution, and high cost of spatial light modulators are currently significant limitations to optical computing and pattern recognition.

Some spatial light modulators have a pixelated structure whereas others are nonpixelated. The pixelated devices may be better suited for optical computing applications because of the ability to address each pixel independently, forming a two-dimensional array of logic elements. However, the pixelated devices have limited use for pattern recognition/image processing applications because the electrode grid structure of the pixelated array yields higher diffraction orders which are difficult to utilize in the Fourier transform plane. Furthermore, the electrode grid structure diminishes the effective area of the modulator which decreases the optical efficiency of the pattern recognition process being performed. Therefore, pixelated SLMs may be better suited for some optical computing applications while nonpixelated ones may be better for pattern recognition applications.

Several modulators have been constructed in recent years which potentially overcome some of the limitations of the most well-known modulator, the Liquid Crystal Light Valve (LCLV) [1]. The more recent devices include a Modified Liquid Crystal Television (MLCTV) [2], the Litton/Semetex Corporation Magneto-Optical Spatial Light Modulator (MOSLM) [3], Texas Instruments' Deformable Mirror Device (DMD) [4], and a Ferroelectric Liquid Crystal Modulator [5].

This report attempts to present a realistic outlook for the future of optical computing and optical pattern recognition by briefly presenting the basics of promising modulators with regard to their response times, resolution, and cost.

The construction and operating characteristics of the LCLV will be presented first as the baseline of comparison used throughout this report. Thereafter, the construction and operating characteristics of four devices, representative of the current state of the art, are discussed at length and compared to the LCLV. Some novel ideas for SLMs, which have not yet reached the same level of development as the more recent devices discussed in this report, are mentioned in the conclusion.

II. THE LIQUID CRYSTAL LIGHT VALVE (LCLV)

The basic construction of Hughes' LCLV is shown in Figure 1. The LCLV has an incoherent image impressed upon the write side of the device. A coherent light source, such as a laser, is used to illuminate the incident read side of the device. The light reflected from the read side of the dielectric mirror contains a coherent image of the originally incoherent image source.

This device is composed of a Cadmium Sulfide (CdS) photoconductive surface followed by a Cadmium Telluride (CdTe) light absorbing layer on the input side, commonly referred to as the write side, of the device. A dielectric mirror is positioned directly against the CdTe layer. The liquid crystal layer is then placed toward the read side of the device between two inert insulating layers of SiO_2. The above assembly, from the CdS photoconductor to the inert insulating layer on the read side of the device, is then sandwiched between two transparent electrode surfaces deposited on optically flat glass.

Typical operation of the LCLV requires the application of a low ac voltage ($\approx$4-10 V) at about 1-5 kHz across the electrodes. The combination of the CdS and CdTe layers creates a junction diode. The dielectric mirror serves three useful purposes. The mirror combined with the CdTe light absorbing layer separates the photoconductor from the read light thereby allowing for the simultaneous writing and reading of the device. Secondly, the dielectric mirror prevents the flow of dc current through the device thus prolonging the useful life of the LCLV. Finally, the reflectivity of the device can be maximized by coating the mirror for any portion of the visible spectrum desired. [6]

The most fundamental component of the LCLV is the liquid crystal layer. The liquid crystal layer ($\approx$2 μm thick) is operated in what is commonly referred to as a hybrid field effect mode. The hybrid field effect mode utilizes conventional twisted nematic electro-optic effect in the off-state (i.e., when no voltage is applied) and optical birefringence effect for the on-state of the liquid crystal. The implementation of the hybrid field effect mode requires the construction of the liquid crystal layer such that the liquid crystal molecules are preferentially aligned with the electrode surfaces. The preferentially twisted alignment is obtained by orienting the electrode surfaces "so that the direction of liquid crystal alignment on the two electrode surfaces makes an acute angle with respect to each other." [6] The twisted alignment causes the polarization of the incident light to rotate by an angle equivalent to the twist angle. The Hughes' LCLV twists the molecules by a 45° angle. An analyzer is then used in the reflected read beam of the device to provide an amplitude- or phase-modulated image of the incident incoherent image.

The operation of the LCLV can be more easily understood if a crossed polarizer/analyzer pair is placed between the LCLV and the source of the read light such that the polarizer is in the incident read beam and the analyzer is in the reflected read beam (see Figure 2). Linearly polarized light which is incident on the LCLV will be twisted by a 45° angle on its first pass through the liquid crystal layer. The light will then be twisted in the opposite direction by 45° when returning through the liquid crystal layer after reflection off the dielectric mirror. Therefore, the exiting

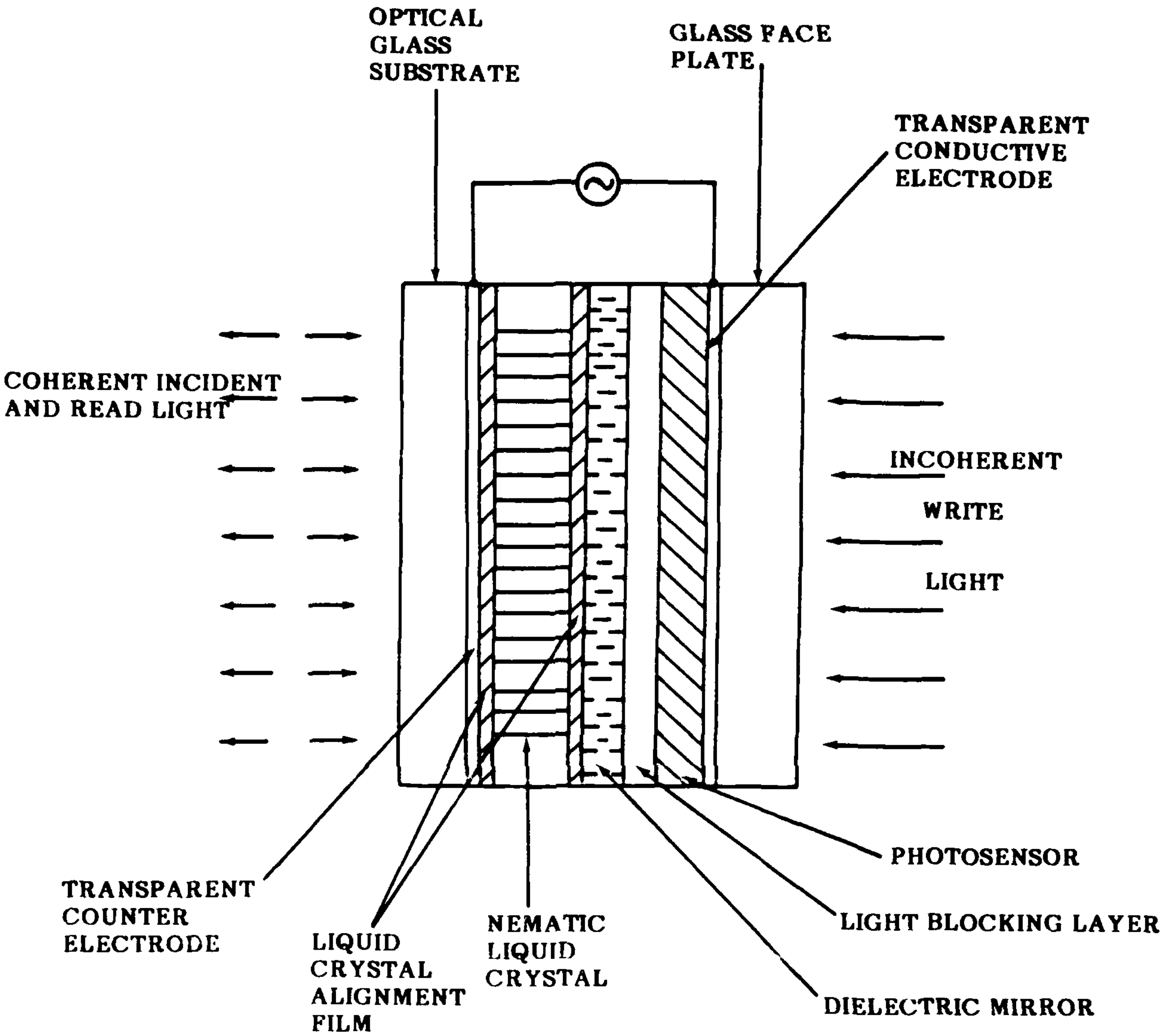

Figure 1. Side view of a liquid crystal light valve.

NOTE: From Reference [6]

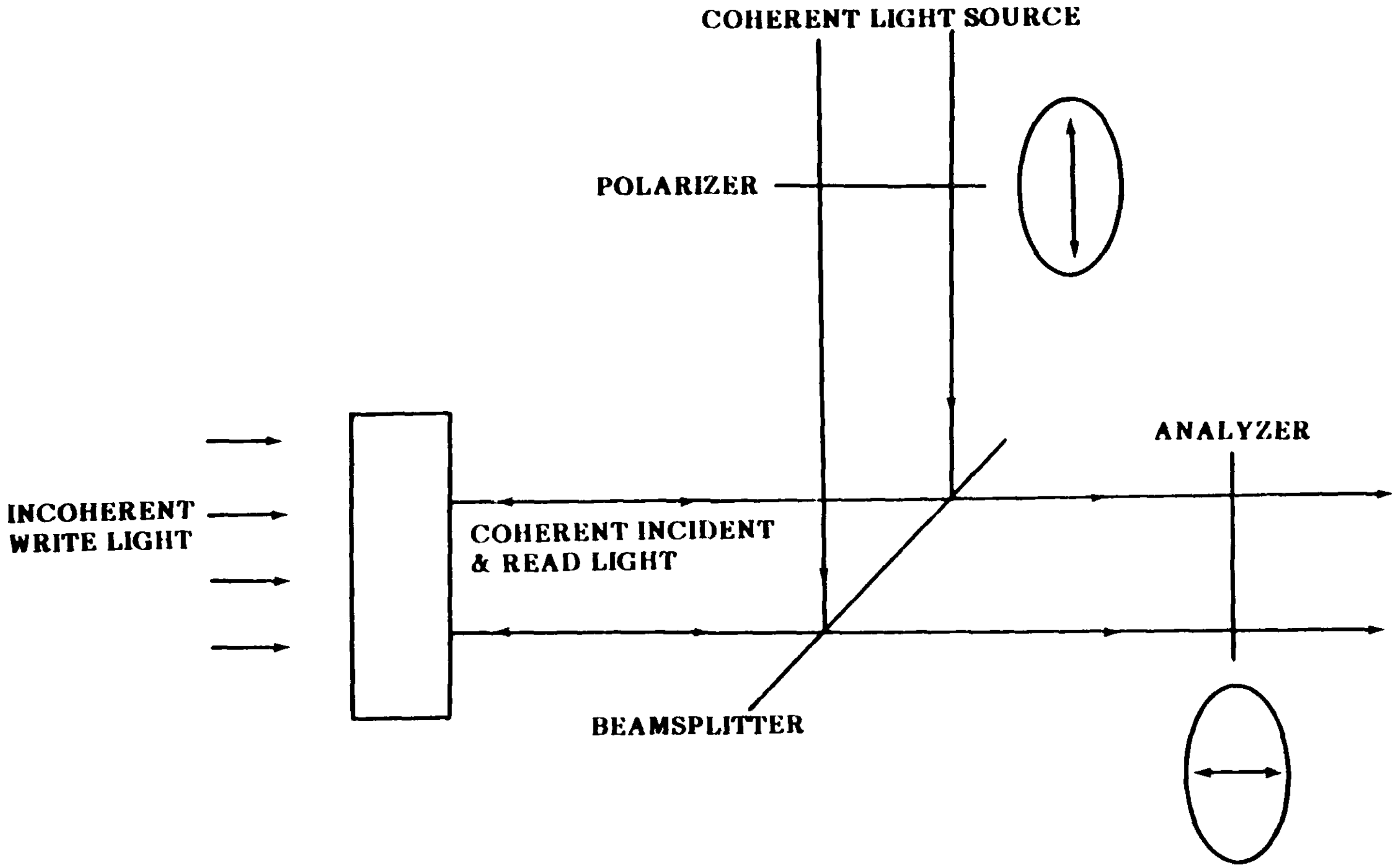

Figure 2. Operation of the LCLV with a crossed polarizer/analyzer pair.

light will be in phase with the incident light which would be blocked by the crossed analyzer. This dark field off-state of the device is logically explained by the twisted nematic effect. Care is exercised so that experimentally the polarization of the incident light entering the read side of the device is aligned along the preferential direction of the electrode surfaces in order for the twisted nematic off-state to work properly.

The polarization of the light can also remain unchanged by the application of a voltage across the electrodes which rotates the liquid crystal molecules such that the long axis of the molecules are oriented perpendicularly to the electrode surfaces. This condition would result in a dark on-state but would be of little value. However, this analogy is important to understand that an applied voltage between the full "on" and full "off" state exists such that the LCLV will transmit light through the analyzer. The liquid crystal molecules affect the polarization of the read light through optical birefringence when the orientation of these molecules is between a horizontal and perpendicular alignment with the electrodes. This occurs for some intermediate voltage between the full "on" and full "off" states.

The performance characteristics for the Hughes' LCLV have been reported as: resolution of 60 lp/mm, a write-and-erase cycle of $\approx$25 ms, input sensitivity of 160 $\mu W/cm^2$, and nine gray scale levels. [6] However, actual experimental use of such a device provided a maximum resolution of 20 lp/mm and an optimal write-and-erase cycle of $\approx$50 ms. Furthermore, the more recent Hughes' LCLVs fabricated have a resolution of 10-20 lp/mm, response times of $\approx$100 ms, and a present cost of approximately $30,000.

III. THE AMORPHOUS SILICON SPATIAL LIGHT MODULATOR

A variation of the Hughes' LCLV which shows great promise is the amorphous silicon (ASi) spatial light modulator reported by Ashley and Davis. [7] The cadmium sulfide layer of the LCLV allows for reasonable resolution but is slow and has a low overall input sensitivity. Crystalline silicon, on the other hand, is fast-acting with good input sensitivity but normally has low spatial resolution due to the thickness required. The amorphous silicon modulator essentially has the cadmium sulfide photoconductor in Hughes' LCLV configuration replaced by an amorphous silicon layer $\approx$5 μm thick. The use of amorphous silicon provides high resolution while maintaining the speed and sensitivity of crystalline silicon. Ashley and Davis reported a resolution greater than 35 lp/mm while achieving an input sensitivity of $\approx$ 20 $\mu W/cm^2$ with their device. [7] Figure 3(a) shows a schematic representation of this device. Response times on the order of a millisecond are expected using the configuration of this SLM.

Furthermore, Ashley, Davis, and Tae Kwan Oh have recently fabricated an amorphous silicon SLM which is optically transmissive. The transmissive ASi SLM, shown in Figure 3(b), is similar in construction to the device in Figure 3(a). The transmissive ASi SLM device incorporates a novel electrode design, located between the photoconductor and the liquid crystal, to increase the efficiency of the field switching which allows for the use of a thin (<1 μm) ASi layer to achieve good optical transmission. Furthermore, the center electrode structure, consisting of aluminum strips approximately 2500 Angstroms thick, generates a two-dimensional field profile in the ASi in the area between the strips. This profile results in an enhanced contrast between the

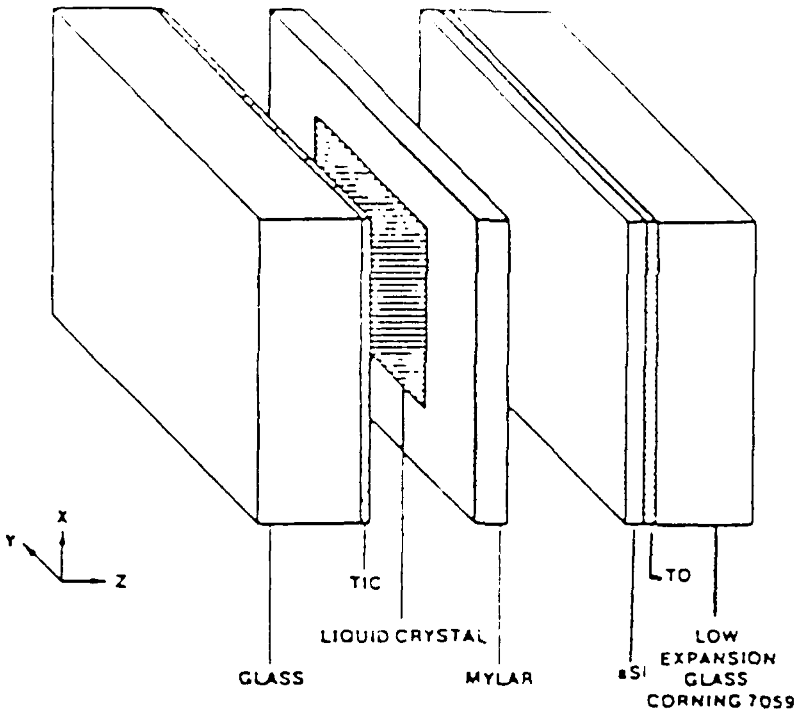

(a) Reflection-type

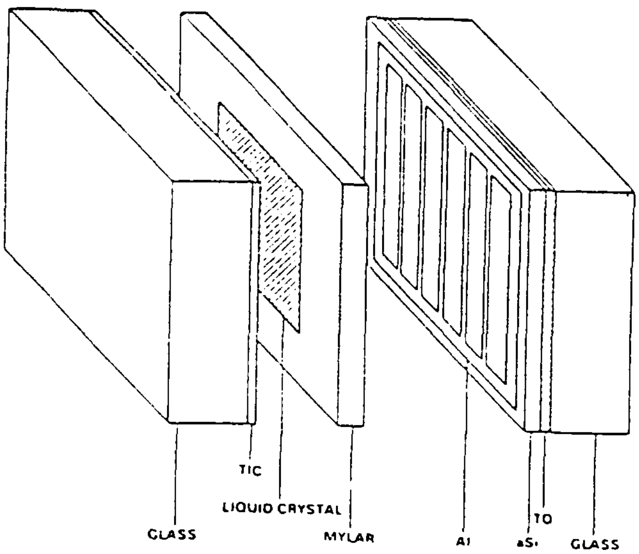

(b) Transmission-mode

Figure 3. Schematic of the amorphous silicon spatial light modulators.

on and off state of the SLM. The electrode strips in this device are 12.5 μm wide with a gap spacing from 12.5-100 μm wide. This SLM was tested with a HeNe read light and a tungsten white light source for writing. These light sources were coaxially aligned with a beamsplitter. Spatial resolution was observed to be greater than 25 lp/mm with a threshold sensitivity of <3 $\mu W/cm^2$. The arrangement of the aluminum strips as vertical bars will of course produce a horizontal diffraction pattern in the Fourier transform plane. This may be disadvantageous if light efficiency is a primary concern.

IV. THE MODIFIED LIQUID CRYSTAL TELEVISION (MLCTV)

In recent years, small inexpensive Japanese-made Liquid Crystal Televisions (LCTV) have been widely used in optical processing experiments because of their ease of operation and video frame rate processing speeds. [8-9] The liquid crystal television is normally viewed by opening a hinged structure which supports the liquid crystal layer sandwiched between two polarizers at a 45° angle with respect to the base. This angle allows ambient room light to transmit through the liquid crystal layer and the television image is viewed by looking at the reflected light from a mirror located on the base. The hinge structure is modified to a 90° angle for optical processing purposes so the liquid crystal display can be utilized in a transmissive mode. This modification also requires the removal of the frosted glass used to diffuse the incident ambient light. Furthermore, the inexpensive polarizers attached to the display were removed and replaced with better quality polarizers in the experimental arrangement.

The basic principles governing the operation of the Modified Liquid Crystal Television (MLCTV) are similar to those of the reflection-type LCLV discussed in section II of this report. However, the twist angle of the MLCTV is 90° versus the 45° angle of the reflection-type LCLV. This is necessary due to the fact that the light passes only once through the liquid crystal television display whereas the incident read light of the LCLV passes through the liquid crystal layer twice. Furthermore, the MLCTV is electrically addressed whereas the LCLV is optically addressed. The electrode addressing structure of the MLCTV produces an array of 148 x 128 pixels. Each pixel is $\approx$370 μm x 370 μm square. A photograph of the modified liquid crystal television and its pixel structure is shown in Figure 4.

Figure 5 schematically shows the operation of the MLCTV's liquid crystal layer. When no electric field is present, the twisted liquid crystal molecules rotate the plane of polarization by 90° and a dark off-state occurs. Conversely, when an electric field of sufficient strength is present, the crystals align with the field, thus having no effect on the plane of polarization of the incident light.

The MLCTV has been shown to be a viable candidate for optical computing [10] and optical pattern recognition [2] applications. The response time of this device is video frame rate ($\approx$33.3 ms), resolution is comparable to some LCLVs, and the unit cost is approximately $30-$200.

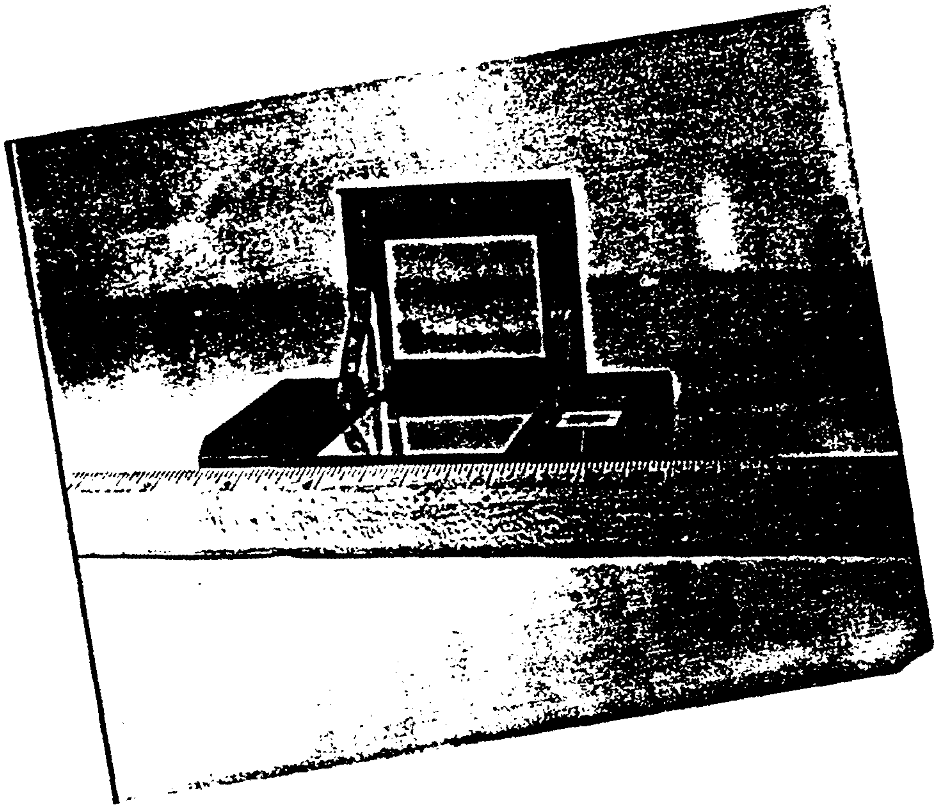

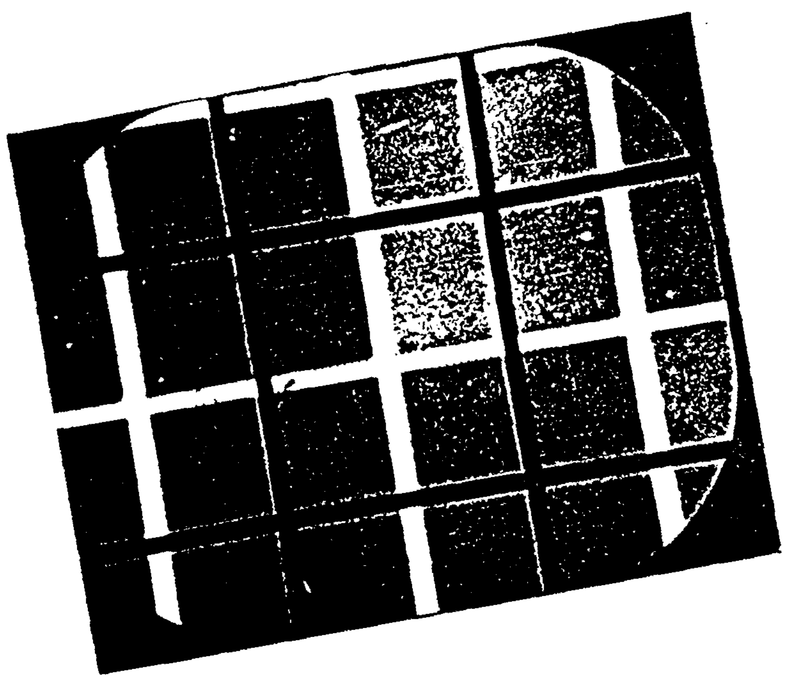

pixel structure: 370 μm x 370 μm

Figure 4. Photograph of the modified LCTV and its pixel structure.

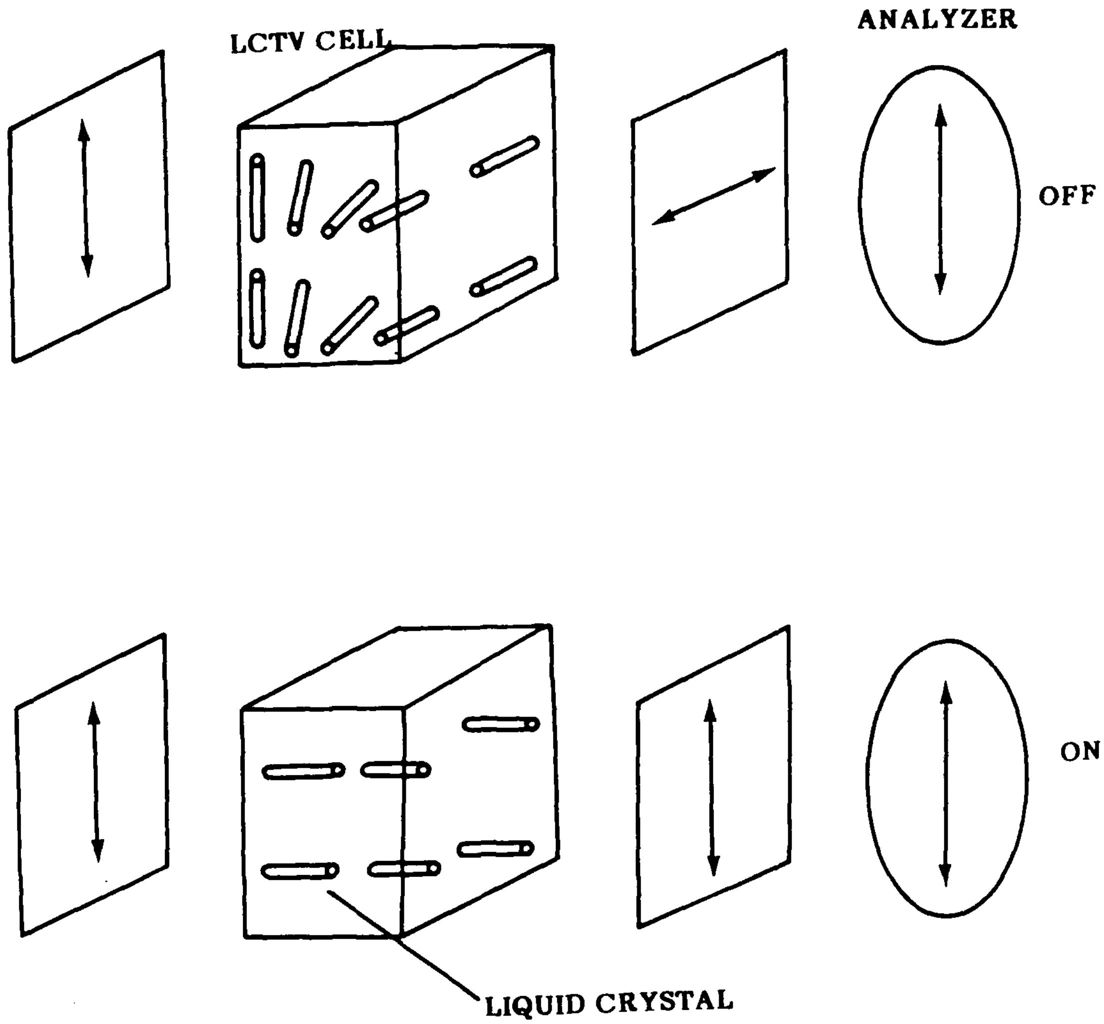

Figure 5. Operation of the modified LCTV's liquid crystal layer.

NOTE: From Reference [10].

V. THE MAGNETO-OPTIC SPATIAL LIGHT MODULATOR (MOSLM)

Another promising candidate for real-time spatial light modulation is the magneto-optic spatial light modulator developed by Litton and Semetex. [11] The MOSLM is a partially transparent array of pixels on a semiconductor chip. Each pixel is made of a magnetic film that exhibits binary (left or right) Faraday rotation of polarized light. Figure 6 schematically shows the binary optical modulation of a pixel via the Faraday effect. Each pixel is $\approx 58\ \mu m \times 58\ \mu m$ square and the current generation of the MOSLM consists of a 128 x 128 pixelated array which has an effective surface area of approximately 1 cm^2. Furthermore, each pixel has an ion implanted corner so as to be especially susceptible to a magnetic field (see Figure 7).

The polarity of each pixel can be controlled by means of currents driven through a grid of conductors surrounding the pixels and the aid of an externally applied magnetic field. The MOSLM is operated by simultaneously driving currents through two orthogonal lines. A strong field is produced at their intersection thus setting the polarity of the implanted corner on the nearest pixel. The magnetic domain of the new state expands to cover the whole pixel with the aid of an externally applied magnetic field from a coil surrounding the semiconductor chip. [12]

A 128 x 128 pixelated device with driver electronics and operating software from Semetex currently costs $18,500. The projected future cost is anticipated to be comparable to present semiconductor chips of comparable size due to the device's semiconductor-based technology. However, the optical efficiency of the MOSLM is very low with only five to seven percent of the incident light being transmitted through the device. Litton and Semetex are currently conducting research to remedy this problem but no concrete evidence of an improvement is presently available. Furthermore, the trade-off between operating speed and power dissipation has not received much attention. Litton and Semetex have estimated cycle times of upwards of 10,000 frames/second for the current generation of the devices. However, ohmic energy of 0.4 μJ to 0.8 μJ is dissipated for each pixel switched and a total of 1 W dissipated in the thin film is sufficient to overheat the commercially available devices. Therefore, an upper limit of 70 frames/second is established for the commercial MOSLM. The operating software, however, actually limits the response time further. Another impedance to the response time is the delay required for the magnetic field produced by the field coil to reach a sufficient operating level.

The MOSLM is a fragile device. This is evident by the limitation placed on the power dissipated through the chip. The fly-wire bonding of the electrodes to the semiconductor chip is also a fragile design which can withstand only minor vibrational shocks. By examination of Figure 8, which shows a magnified view of these bonds, the delicacy of the device is readily apparent.

The MOSLM costs only 2/3 the price of the Hughes LCLV. Resolution of the device is limited due to binary representation via a pixelated array of an image. Figure 9 shows an amplitude-modulated image on the 128 x 128 pixelated device using a HeNe laser for illumination. Although current response times are not as fast as the LCLV, the theoretical limit of 70 frames/second compares favorably to the 20 frames/second achieved by the LCLV. Skepticism

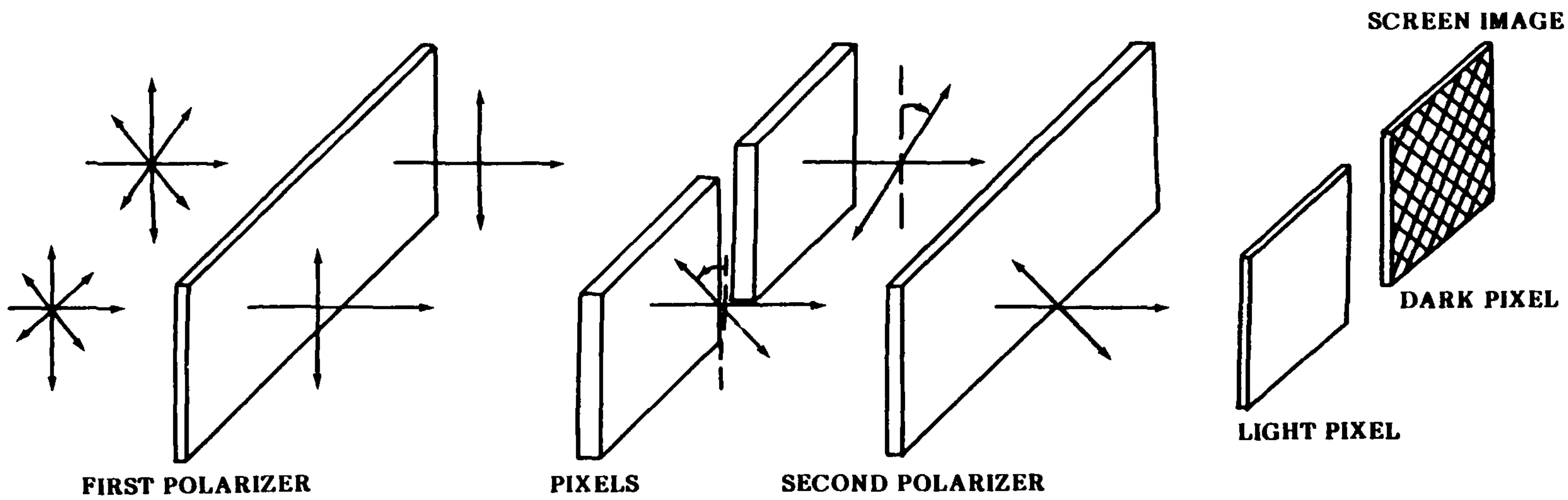

Figure 6. <u>Optical modulation via the magneto-optic Faraday effect</u>.

NOTE: From Reference [3].

abounds about the future utilization of the MOSLM for widespread optical computing, but the device may be a suitable candidate for limited applications in optical pattern recognition and tracking.

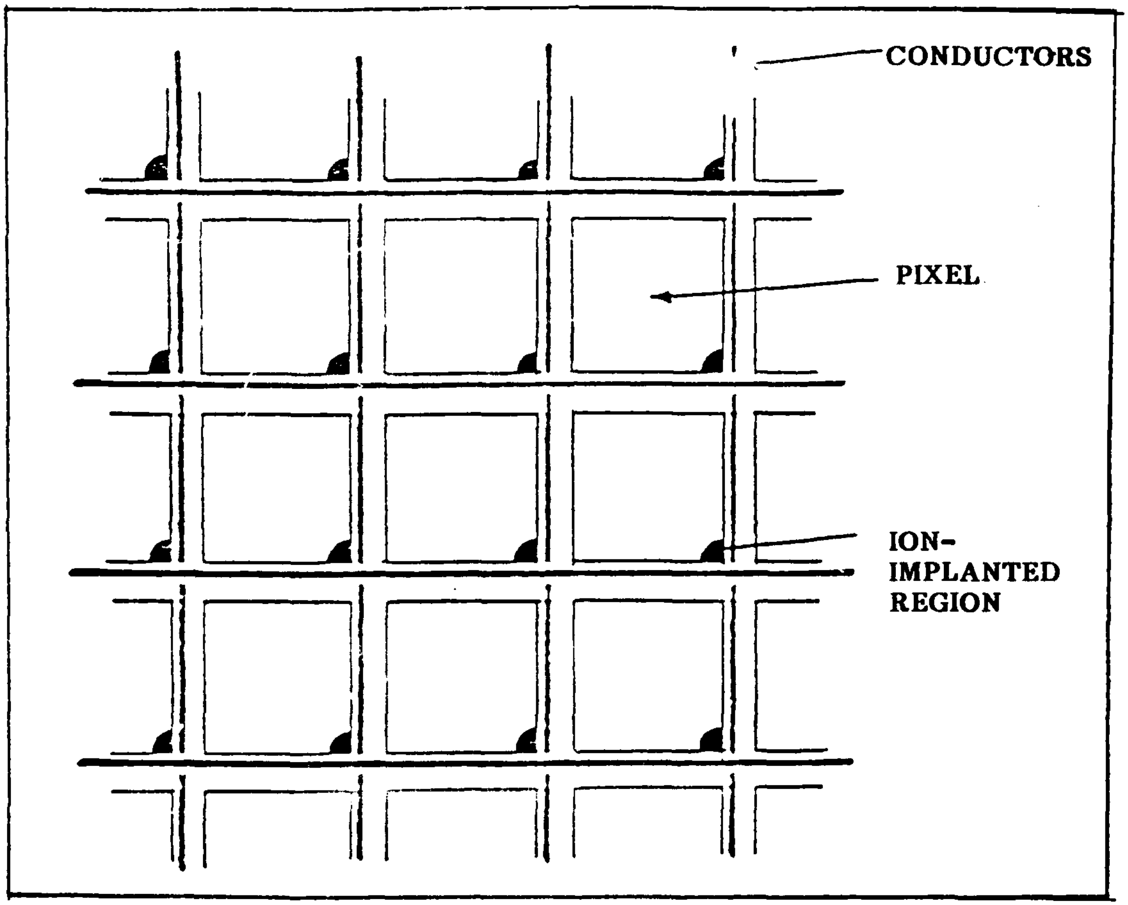

Figure 7. Representation of the pixel structure of the MOSLM.

NOTE: From Reference [12].

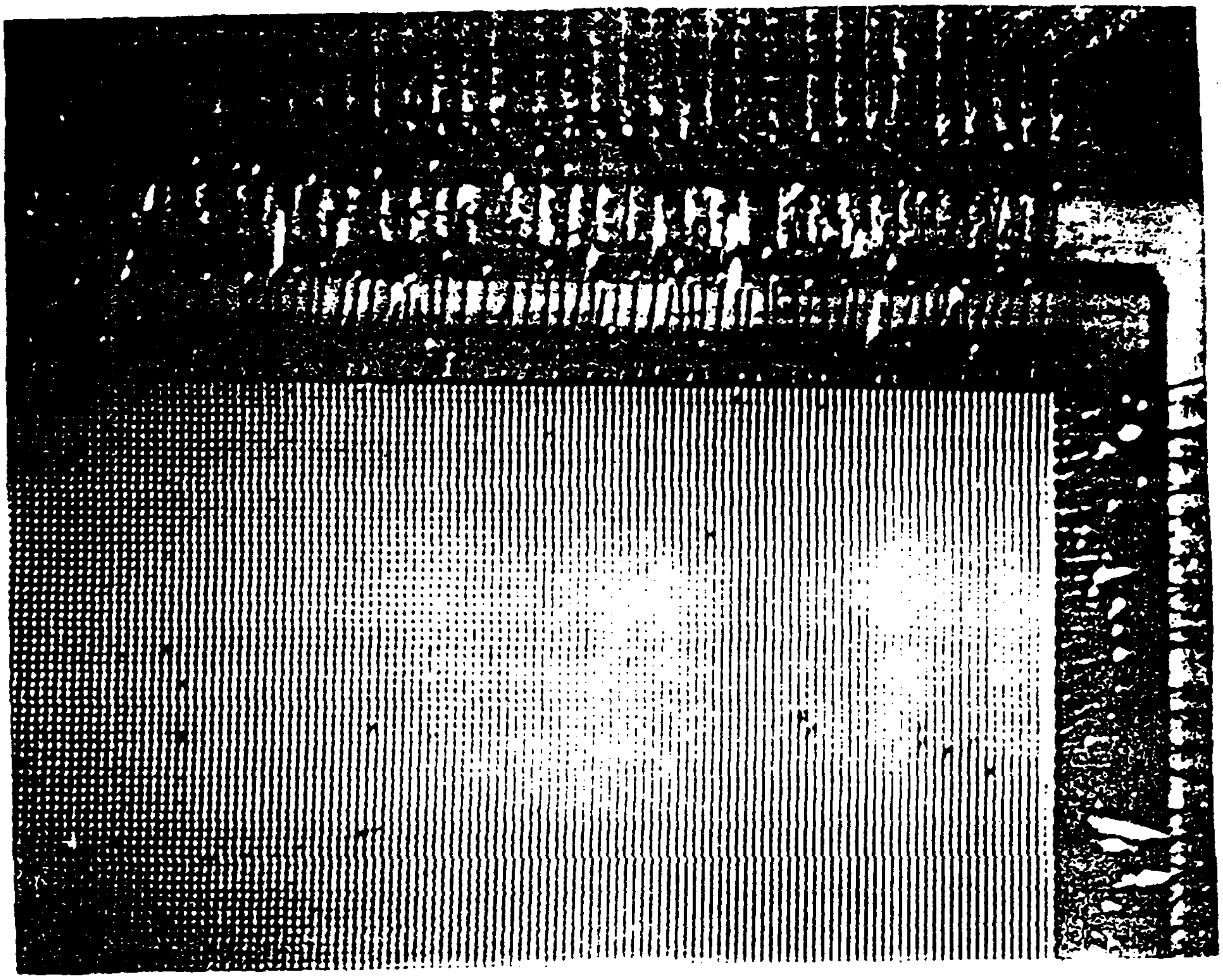

Figure 8. Magnified view of the MOSLM's fly-wire bondings to the semiconductor chip.

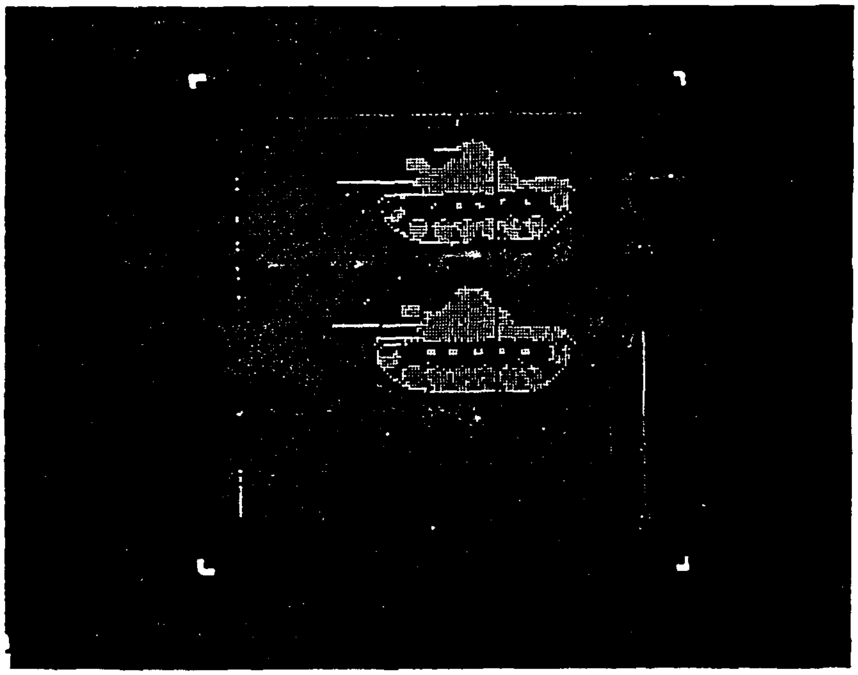

Figure 9. An amplitude-modulated image displayed on a 128 x 128 pixelated MOSLM.

VI. THE DEFORMABLE MIRROR DEVICE (DMD)

A deformable mirror device developed by Texas Instruments Corporation has also shown some promise as a spatial light modulator for optical computing applications. [13] Typical response times of deformable materials are in the μs range whereas the response times of liquid crystals are typically in the millisecond range. Two types of deformable devices have been explored by Texas Instruments. One of these devices is an optically-addressable deformable membrane device and the other is an electrically-addressed Deformable Mirror Device (DMD). The optically addressed membrane device reported by Pape [14] only worked briefly and comparable results have not been produced with future attempts. The electrically-addressed DMD appears to be a much more viable candidate as a spatial light modulator.

The DMD consists of an array of mirrors which deflect into underlying wells according to the electrical signal applied to the device. This electrical signal is supplied from a video input. A coherent read light is used to illuminate the surfaces of these mirrors and the reflected light beam contains a phase-modulated image of the original video input scene. The two-dimensional array of air gap capacitors/mirrors overlay a support structure of square wells etched ≈ 0.7 μm deep. Four mirrors are hinged at the corners of each pixel which are defined by the wells with openings of 20 μm x 20 μm (see Figure 10). The underlying support structure is an analog silicon address circuit which is electronically addressed by an array of MOS transistors. Figure 11 shows a perspective view of this device.

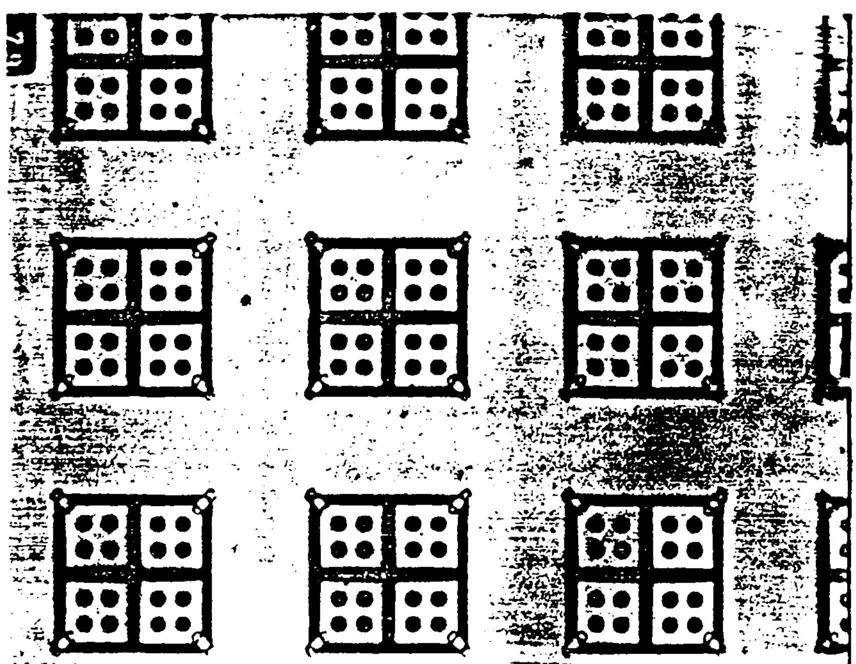

Figure 10. The deformable mirror device's front surface mirrors.

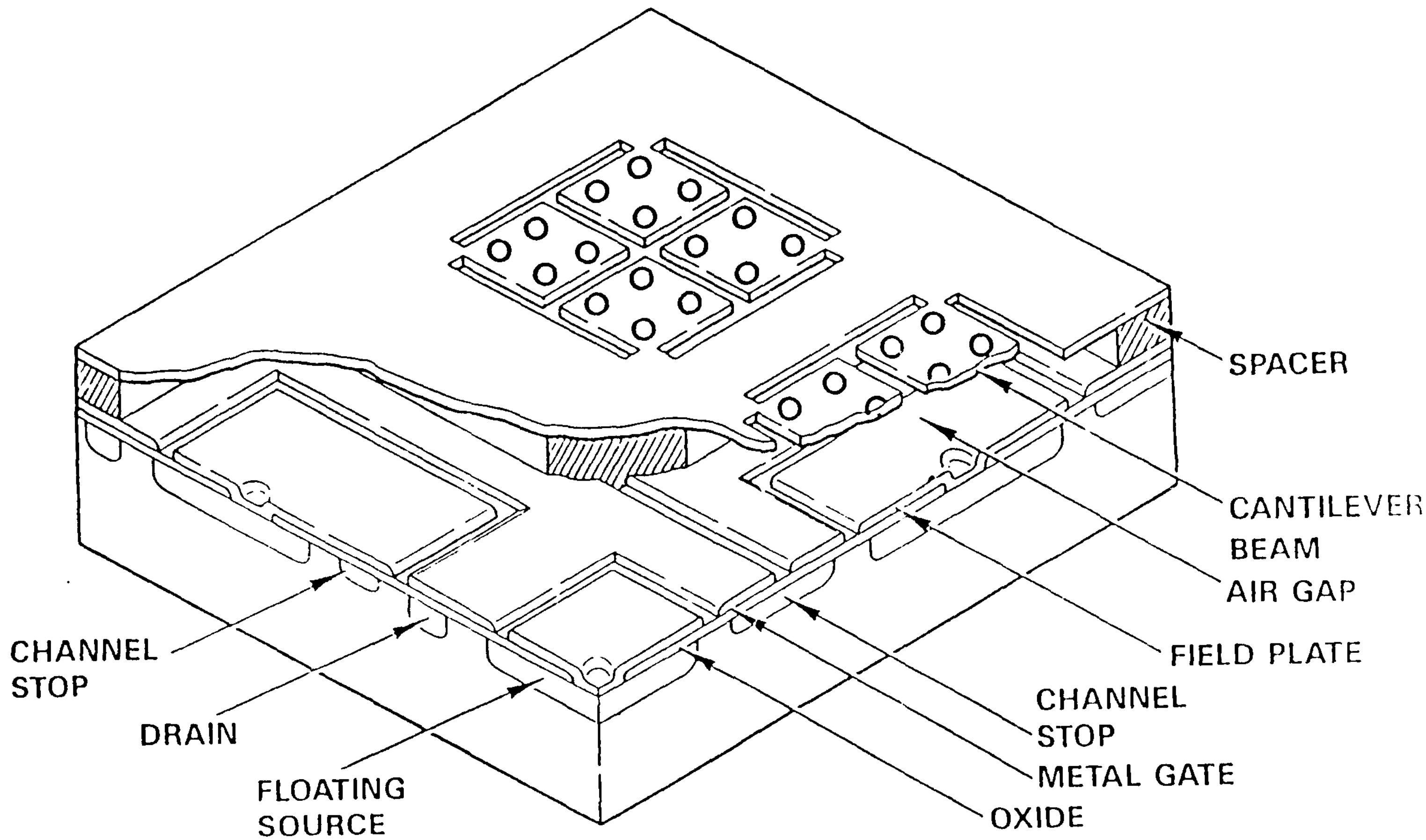

Figure 11. Perspective view of the deformable mirror device.

The addressing organization of the DMD is shown in Figure 12. The operation of the device consists of serially clocking in lines of video into a serial/parallel (S/P) converter. Each clocked line is then parallel dumped onto storage registers so the next line of video can be clocked. The drain lines of the MOS transistors, which are connected to the S/P converter, are charged to voltage levels representative of the contents of the storage registers while the succeeding line of video is being clocked in by the S/P converter. A decoder then momentarily activates the gates of the transistors so the line of video can be stored in the air gap capacitor elements. The above process is continued for each video line. The charge stored in each air gap capacitor causes the array of mirrors to be displaced into the well by an electrostatic force. This deformation is proportional to the voltage level intensity of the stored video data and the displacement pattern yields a phase-modulated image when read with a reflected beam of light. [15]

The amount of time required for each video line to settle is determined by the mechanical response of the mirrors which has been experimentally measured to be ≈ 25 μs. Projected operating speeds of the device are in the neighborhood of 7,000 frames/second. [16] The first-order diffraction efficiency of the Fourier transform of a phase-modulated image has been measured to be 8.4 percent. [17] The resolution of the DMD is limited by its 128 x 128 pixelated array with each pixel etched on 51 μm centers. Figure 13 shows a checkerboard image produced by the DMD in a Schlieren projection system. The present devices do not have the decoders or a serial/parallel converter directly on the chip but future designs are to include these elements on-chip. The major source of defects observed with the operation of the DMD is due to particle contamination between the mirrors and the silicon address circuit which has resulted in some nonfunctional pixels.

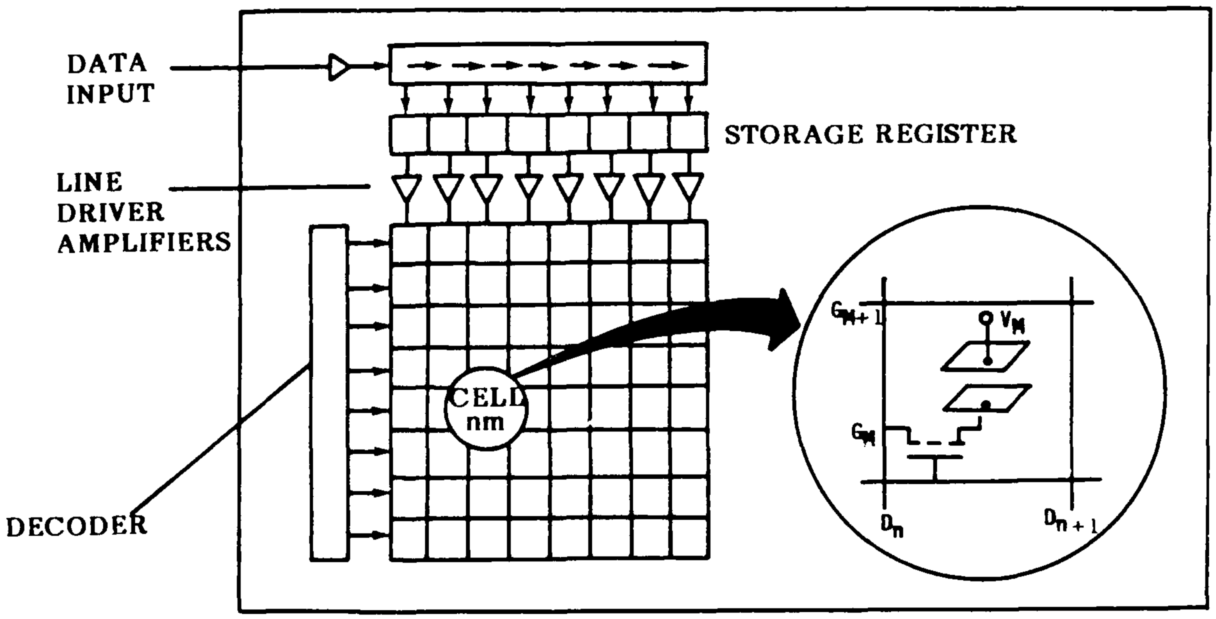

Figure 12. The addressing organization of the DMD.

NOTE: From Reference [4].

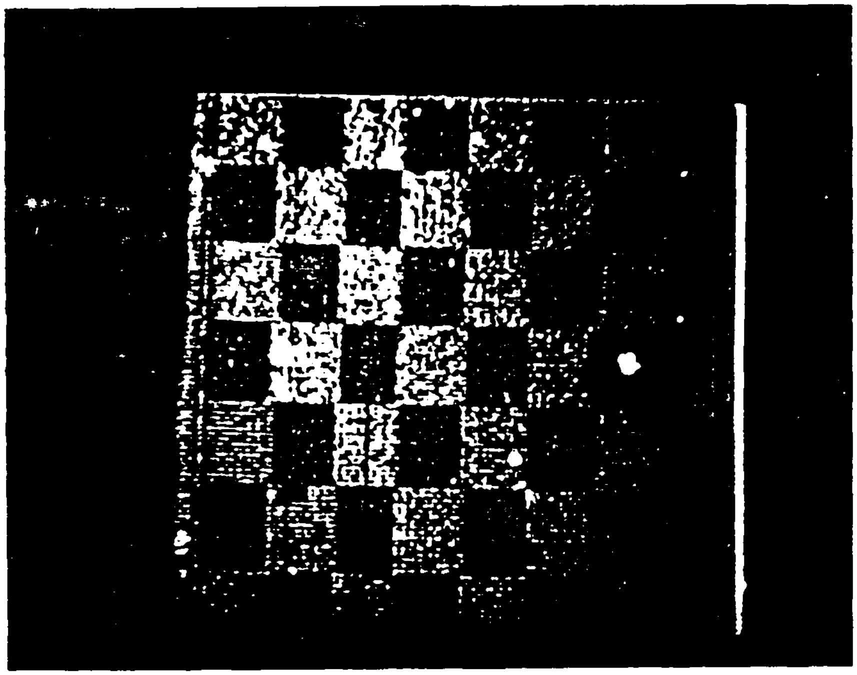

Figure 13. The image of a checkerboard pattern using the DMD in a Schlieren projection system.

The DMD is still in the development stages and is not readily available on a mass production basis. However, the response time of the DMD is significantly greater than that of a LCLV and the cost of the device should be lower than Hughes' LCLV. This is due to the VLSI semiconductor technology employed in the addressing circuit.

Another solid-state SLM which is commercially available is Hamamatsu Corporation's microchannel spatial light modulator (MSLM). The MSLM consists of a photocathode, a microchannel plate (MCP), and a $LiNbO_3$ crystal. [18] Figure 14 shows how the MSLM operates. An incoherent image is input to the photocathode where it is converted to a photoelectron image. An electric charge image is then deposited on the surface of the $LiNbO_3$ crystal after approximately 10^3 electron multiplication by the microchannel plate. These electric charges modify the electric field across the crystal thereby modulating the refractive index of the crystal. By illuminating the crystal from behind with polarized coherent light, a phase shift of the reflected coherent light is induced. Then, by using an analyzer, a coherent optical image corresponding to the input image is obtained. Hamamatsu Corporation reports a spatial resolution of 10 lp/mm, an input sensitivity of 30 nJ/cm^2, and a response time of approximately 100 ms. Furthermore, the MSLM has preprocessing functions capable of performing image addition and subtraction, edge enhancement, and logic operations. The cost of this device is approximately \$25,000-\$30,000.

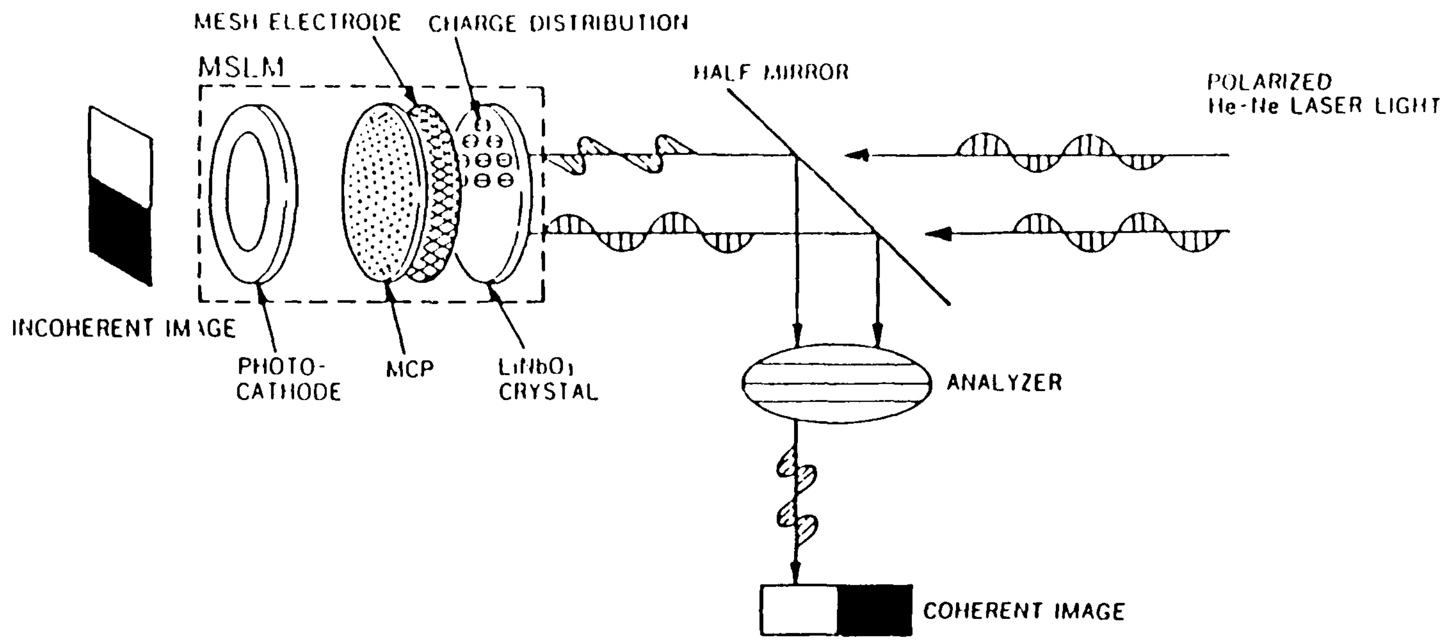

Figure 14. Operating principle of Hamamatsu's microchannel MSLM.

VII. FERROELECTRIC LIQUID CRYSTAL MODULATOR (FLCM)

The ferroelectric liquid crystal has recently been considered as a candidate for optical computing applications. [19] The electro-optical modulation of the material occurs when voltages of opposite signs are applied to two electrode-coated glass plates which sandwich a slab of Ferroelectric Liquid Crystal (FLC). The voltages selected will determine the optical axis orientation which can assume one of two possible forms, both of which are parallel to the glass plates and differ by an angle equivalent to twice the tilt angle of the ferroelectric material. The tilt angle of most ferroelectric materials is 22.5° over a wide range of temperatures. Therefore, the optical axis is electrically rotated by an angle of 45°. [5]

Figure 15 illustrates the electro-optical modulation of a ferroelectric liquid crystal element. The polarization of the FLC is chosen so the incident light is either parallel or perpendicular to one of the voltage-selected optical axis orientations so the light will be transmitted through the cell unaffected. However, if the voltage state is changed to a voltage of equal magnitude but opposite polarity, then the optical axis is rotated by 45° from the incident polarization. The thickness of the material is chosen so a total phase shift of π will occur for light passing through the cell under this condition. Therefore, the incident light's polarization will be rotated by 90° for a dark field effect. Typical voltages used for the modulation of FLC are small ($\approx \pm 16$ V).

A Ferroelectric Liquid Crystal Modulator (FLCM) may consist of an array of FLC pixels. Each pixel is approximately 17 μm x 17 μm square with a 5 μm spacing between each pixel. A 32 x 32 pixelated array has been fabricated and tested by Johnson, et al. [5] The contrast ratio of the device was measured to be 125:1. This ratio can potentially be improved by correcting for the light leakage which occurred through the spacing between pixels. The switching speed of the device is limited by the maximum allowable power dissipation much like the MOSLM discussed in section V of this report. Switching speeds in the microsecond range have been observed with this modulator. Furthermore, the FLCM is useful in optical logic systems due to the stability of the written image. This image can be retained indefinitely by an intrinsic memory once the device is written to with a pulse long enough to switch the state of the FLC (≈ 12 μs). This retention is also observed in the MOSLM previously discussed.

An optically-addressed FLCM is currently being developed by Kristina Johnson and Garrett Moddel at the University of Colorado, Boulder. Unlike the above mentioned electrically-addressed device, this modulator is not pixelated and contains an amorphous silicon photoconductive surface for the operation of the FLC layer similar to the CdS's role in the LCLV's nematic liquid crystal layer discussed in section II of this report. This modulator will only represent an input scene with a binary-modulated image. Estimated cost of the device is $17,500 with a minimum resolution of 30 lp/mm, contrast ratio of 100:1 (possibly greater), and a response time in the microsecond range.

The optically-addressed FLCM would surpass the performance of the Hughes LCLV. For approximately 2/3 the cost of a LCLV, one could expect a device with 50 percent better resolution than the LCLV and response times in the microsecond range as opposed to ≈ 100 ms for a LCLV.

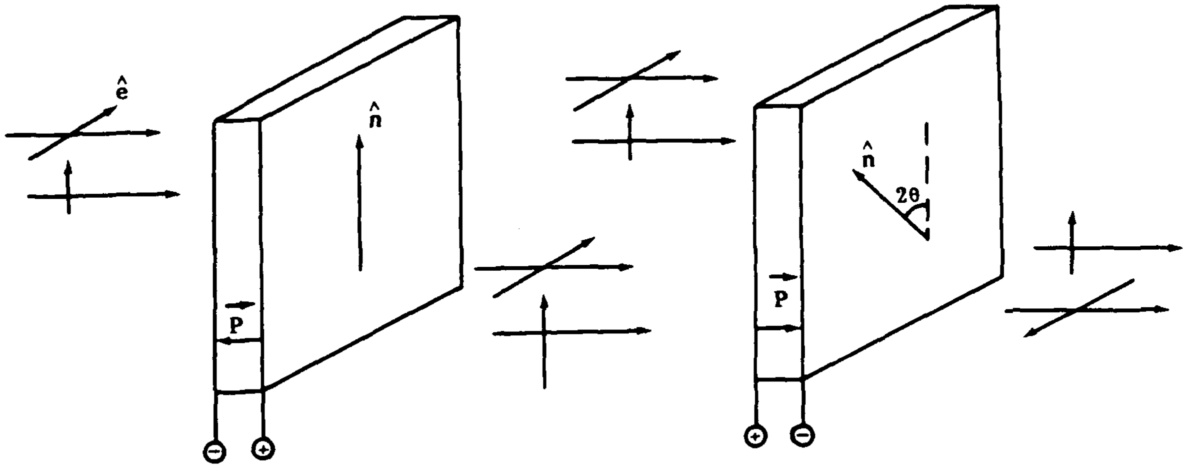

Figure 15. Electro-optical modulation of the ferroelectric liquid crystal.

NOTE: From Reference [5], p 386.

VIII. CONCLUSION

The modulators discussed in this report do not comprise an all inclusive listing but only represent a small percentage of the devices that are being developed or are available. Some other modulators include a silicon/PLZT SLM [20], a photoemitter membrane light modulator [21], a deformable gel surface SLM [22], and a micro-mechanical light modulator [23]. Arthur Fisher and John Lee have published the most inclusive listing of spatial light modulators (SLM) thus far, and yet even this list is not complete. [24] The purpose of such listings is to provide optical designers with the necessary information to select the most effective SLM for their application.

Spatial light modulators are key components in various optical computing, optical pattern recognition, and guidance applications. In the past, few SLMs were widely available, but presently many SLMs are available and more are being developed. Each modulator has advantages and disadvantages depending on the application for which it is to be employed. The SLMs discussed in this report, and summarized in Figure 16, are being investigated by the U. S. Army Missile Command's Research, Development, and Engineering Center, Research Directorate located at Redstone Arsenal, Alabama for use in optical correlating applications such as pattern recognition and tracking.

The forefront of SLM technology is on the verge of an explosion of viable devices for all sorts of optical processing applications. The ferroelectric modulator and the deformable mirror device appear to be leading this assault. All indications point to the probability that a library of high-resolution, fast-response, cost-effective SLMs will be available in the near future for the optical designer to choose from for his intended application.

SPATIAL LIGHT MODS	COST	RESOLUTION	RESPONSE
1. HUGHES' LCLY (CdS)	$30-40K	10-20 lp/mm	100 milliseconds
2. Amorphous Silicon SLM	Being developed	>35 lp/mm	few milliseconds (projected)
3. Modified LCTY	$100.00	148 x 128 pixels (each pixel 370 μm on the sides)	33.3 milliseconds
4. Magneto-optic SLM	$18.5K	128 x 128 pixels (each pixel 58 μm on the side)	14 milliseconds (70 frames/sec)
5. Deformable Mirror Device	Being developed	128 x 128 pixels (each pixel 51 μm on the side)	1 microsecond (projected)
6. Mircochannel SLM	$25-30K	10 lp/mm	150 milliseconds
7. Ferroelectric LC SLM	$17.5K (estimated)	>30 lp/mm (projected)	1 microsecond (estimated)

Figure 16. Summary of SLMs and key operating parameters.

REFERENCES

1. Yu, Francis T. S., Optical Information Processing, New York: John Wiley and Sons, 1983, pp. 134-137.

2. Gregory, D. A., "Real-Time Pattern Recognition Using a Modified Liquid Crystal Television in a Coherent Optical Correlator," Applied Optics, Vol. 25, pp. 467-469, February 15, 1986.

3. Ross, W. E., Psaltis, D., and Anderson, R. H., "Two-Dimensional Magneto-Optic Spatial Light Modulator for Signal Processing," Optical Engineering, Vol. 22 , No. 4, pp. 485-490, July/August 1983.

4. Pape, D. R. and Hornbeck, L. J., "Characteristics of the Deformable Mirror Device for Optical Information Processing, "Optical Engineering, Vol. 22, No. 6, pp. 675-681, November/December 1983.

5. Johnson, K. M., Handschy, M. A., and Pagano-Stauffer, L. A., "Optical Computing and Image Processing with Ferroelectric Liquid Crystals," Optical Engineering, Vol. 26, No. 5, pp. 385-391, May 1987.

6. Grinberg, J., Jacobson, A., Bleha, W., Miller, L., Fraas, L., Boswell D., and Myer, G., "A New Real-Time Non-Coherent to Coherent Light Image Converter the Hybrid Field Effect Liquid Crystal Light Valve," Optical Engineering, Vol. 14, No. 3, pp. 217-223, May/June 1975.

7. Ashley, P. R. and Davis, J. H., "Amorphous Silicon Photoconductor in a Liquid Crystal Spatial Light Modulator," Applied Optics, Vol. 26, No. 2, pp. 241-246, 15 January 1987.

8. Liu, H. K., Davis, J. A., and Lilly, R. A., "Optical-Data-Processing Properties of a Liquid-Crystal Television Spatial Light Modulator," Optics Letters, Vol. 10, No. 12, pp. 635-637, December 1985.

9. Yu, Francis T. S., Jutamulia, S., Lin, T. W., and Huang, X. L., "Real-Time Pseudocolour-Encoding Using a Low-Cost Liquid Crystal Television," Optics and Laser Technology, Vol . 19, No. 1, pp. 45-47, February 1987.

10. Yu, Francis T. S., Jutamulia, S., and Gregory, D. A., "Real-Time Liquid Crystal TV XOR- and XNOR-Gate Binary Image Subtraction Technique," Applied Optics, Vol. 26, No. 14, pp. 2738-2740, July 15, 1987.

11. Ross, W. E., Snapp, K. M., and Anderson, R. H., "Fundamental Characteristics of the Litton Iron Garnet Magneto-Optic Spatial Light Modulator," SPIE Proceedings, Vol. 388.

12. Psaltis, D., Paek, E. G., and Venkatesh, S. S., "Optical Image Correlation With a Binary Spatial Light Modulator," Optical Engineering, Vol. 23, No. 6, p. 698, November/December 1984.

13. Gregory, D. A., Juday, R. D., Sampsell, J., Gale, R., Cohn, R. W., and Monroe, S. E., "Optical Characteristics of a Deformable Mirror Spatial Light Modulator," Optics Letter, Vol. 13, No. 1, pp. 10-12, January 1988.

REFERENCES

14. Pape, D., "Optically Addressed Membrane Spatial Light Modulator," Optical Engineering, Vol. 24, No. 1, pp. 107-110, January/February 1985.

15. Hornbeck, L. J., "128 x 128 Deformable Mirror Device," IEEE Transactions on Electron Devices, Vol. ED-30, No. 5, pp. 539-545, May 1983.

16. Pessoney, S. L., "Coherent Display Characteristics of a Deformable Mirror Spatial Light Modulator," USAMICOM Special Report RD-RE-87-2, p. 105, September 1987.

17. Pape, D. R. and Hornbeck, L. J., "Characteristics of the Deformable Mirror Device for Optical Information Processing," Optical Engineering, Vol. 22, No. 6, pp. 675-681, November/December 1983.

18. Hara, T., Sugiyama, M., and Suzuki, Y., "A Spatial Light Modulator," Advances in Electronics and Electron Physics, Vol. 64B, pp. 637-647 (1985).

19. Patel, J. S., Goodby, J. W., "Properties and Applications of Ferroelectric Liquid Crystals," Optical Engineering, Vol. 26, No. 5, pp. 373-384, May 1987.

20. Lee, S. H., et al., "Two-Dimensional Silicon/PLZT Spatial Light Modulator: Design Considerations and Technology," Optical Engineering, Vol. 25, No. 2, pp. 250-260, February 1986.

21. Fisher, A. D., et al., "Photoemitter Membrane Light Modulator," "Optical Engineering, Vol. 25, No. 2, pp. 261-268, February 1986.

22. Hess, K., et al., "Deformable Surface Spatial Light Modulator," Optical Engineering, Vol. 26, No. 5, pp. 418-422, May 1987.

23. Brooks, R. E., "Micromechanical Light Modulators on Silicon," Optical Engineering, Vol. 24, No. 1, pp. 101-106, January/February 1985.

24. Fisher, A. D. and Lee, J. N., "The Current Status of Two-Dimensional Spatial Light Modulator Technology," Proceedings of SPIE, Vol. 634, pp. 352-371, 1986.

DISTRIBUTION

	Copies
Director U.S. Army Research Office ATTN: SLCRO-PH ATTN: SLCRO-ZC P. O. Box 12211 Research Triangle Park, NC 27709-2211	1
Headquarters Department of the Army DAMA-ARR Washington, DC 20310-0632	1
Headquarters OUSDR&E The Pentagon ATTN: Dr. Ted Berlincourt Washington, DC 20310-0632	1
Defense Advanced Research Projects Agency Defense Sciences Office Electronics Systems Division ATTN: Dr. John Neff 1400 Wilson Boulevard Arlington, VA 22209	1
Commander U.S. Army Foreign Science and Technology Center ATTN: AIAST-RA 220 Seventh Street, NE Charlottesville, VA 22901-5396	1
Director, URI University of Rochester College of Engineering and Applied Science The Institute of Optics Rochester, NY 14627	1
Director, JSOP University of Arizona Optical Science Center Tucson, AZ 85721	1
Electro-Optical Terminal Guidance Branch Armament Laboratory ATTN: Dr. Steve Butler Eglin Air Force Base, FL 32542	1

DISTRIBUTION (Continued)

	Copies
U.S. Army CRREL ATTN: Dr. Richard Munis 72 Lyme Mill Road Hanover, NH 03755	1
Night Vision and Electro-Optics Center ATTN: AMSEL-NV-T, Mark Norton Building 357 Fort Belvoir, VA 22060	1
RADC/ESOP ATTN: Dr. Joseph Horner Hanscom AFB, MA 01731	1
Applied Science Division Applied Optics Operations ATTN: Dr. Robert D. Buzzard P. O. Box 3115 Garden Grove, CA 92641	1
Department of Electrical Engineering Stanford University ATTN: Dr. J. W. Goodman Stanford, CA 94305	1
University of Alabama in Huntsville Center for Applied Optics ATTN: Dr. H. John Caulfield Huntsville, AL 35899	1
University of Alabama in Huntsville Physics Department ATTN: Dr. J. G. Duthie Huntsville, AL 35899	1
Carnegie-Mellon University Department of Electrical and Computer Engineering ATTN: Dr. David Casasent Pittsburgh, PA 15213	1
Penn State University Department of Electrical Engineering ATTN: Dr. F. T. S. Yu University Park, PA 16802	1

DISTRIBUTION (Continued)

	Copies
University of Alabama in Birmingham Physics Department ATTN: Mr. James F. Hawk University Station Birmingham, AL 35294	1
NASA Johnson Space Center ATTN: Code EE-6, Dr. Richard Juday Houston, TX 77058	1
Jet Propulsion Lab ATTN: Dr. Michael Shumate 4800 Oak Grove Drive Pasadena, CA 91109	1
Naval Weapons Center ATTN: Code 3941, David Bloom China Lake, CA 93555	1
University of Colorado at Boulder Department of Electrical and Computer Engineering ATTN: Dr. Kristina Johnson Boulder, CO 80309-0425	1
Naval Research Lab ATTN: Code 6537, Dr. Arthur Fisher Washington, D.C. 20375-5000	1
AMSMI-RD, Dr. McCorkle	1
Dr. Rhoades	1
AMSMI-RD-RE, Dr. J. Bennett	1
AMSMI-RD-RE-OP, Dr. Charles Bowden	1
Dr. Don A. Gregory	1
Mr. David J. Lanteigne	1
Mr. James C. Kirsch	1
Mr. Tracy D. Hudson	80
AMSMI-RD-CS-R	5
AMSMI-RD-CS-T	1
AMSMI-GC-IP	1
DASD-H-V	1